

The First Example of Commensurate Adsorption of Atomic Gas in a MOF and Effective Separation of Xenon from Other Noble Gases

Hao Wang,^a Ke Xin Yao,^b Zhijuan Zhang,^c Jacek Jagiello,^d Qihan Gong,^a Yu Han^b
and Jing Li^{*a}

^a *Department of Chemistry and Chemical Biology, Rutgers University, 610 Taylor Road, Piscataway, New Jersey, 08854, USA*

^b *Advanced Membranes and Porous Materials Center, Physical Sciences and Engineering Division, and Imaging and Characterization Core Lab, King Abdullah University of Science and Technology, Thuwal 23955-6900, Saudi Arabia*

^c *Institute of Atmospheric Environment Safety and Pollution Control, Jinan University, Guangzhou, 510632, China*

^d *Micromeritics Instrument Corporation, 4356 Communications Drive, Norcross, GA, 30093*

*Correspondence should be directed to: jingli@rutgers.edu

Supporting Information

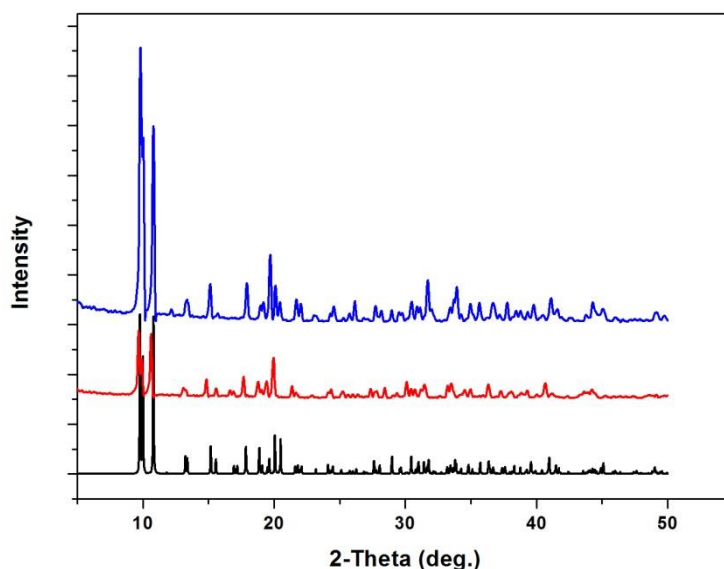
I. Synthesis and structure characterization

Reagents and materials: All chemicals were purchased from Sigma Aldrich, Alfa Aesar and used as received without further purification unless stated otherwise.

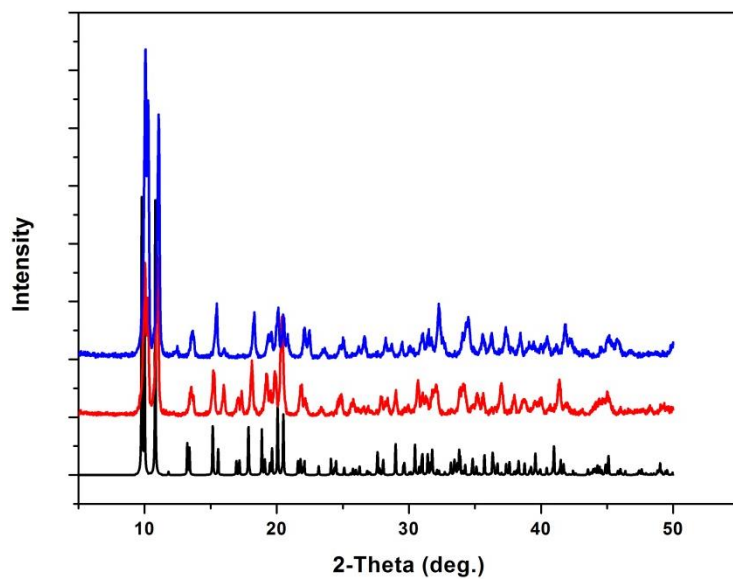
Synthesis of $\text{Co}_3(\text{HCOO})_6$: A mixture of Cobalt (II) nitrate hexahydrate (1.309g, 4.4 mmol) and formic acid (1mL, 25.7mmol) in DMF (10 mL) in a glass vial was heated at 100 °C for 24 hours and then cooled to room temperature. The resultant pink powder of was filtered, rinsed with DMF (10 mL) and dried under air.

Same procedure was employed in the syntheses of other $\text{M}_3(\text{HCOO})_6$ (M=Ni, Mn) compounds.

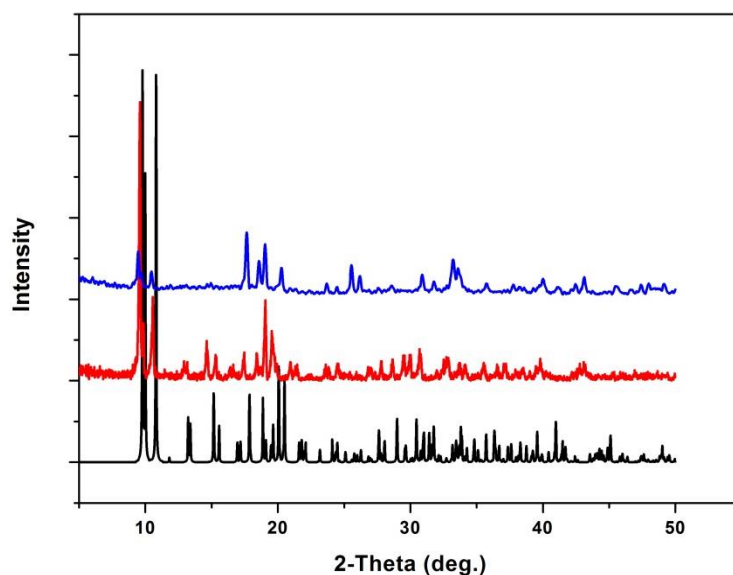
Instrument and method: Powder X-ray diffraction patterns were recorded on a Rigaku D/M-2200T automated diffractometer (Ultima+) using Cu $\text{K}\alpha$ radiation ($\lambda = 1.5406 \text{ \AA}$). Graphite monochromator was used and the generator power settings were at 44 kV and 40 mA. Data were collected between a 2θ of 3-50° with a step size of 0.02° at a scanning speed of 3.0 deg/min.



(a)



(b)

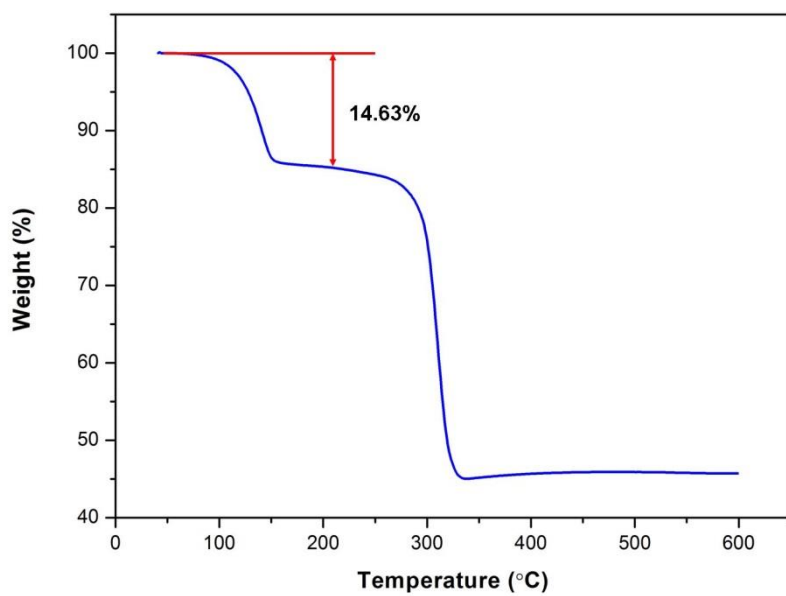


(c)

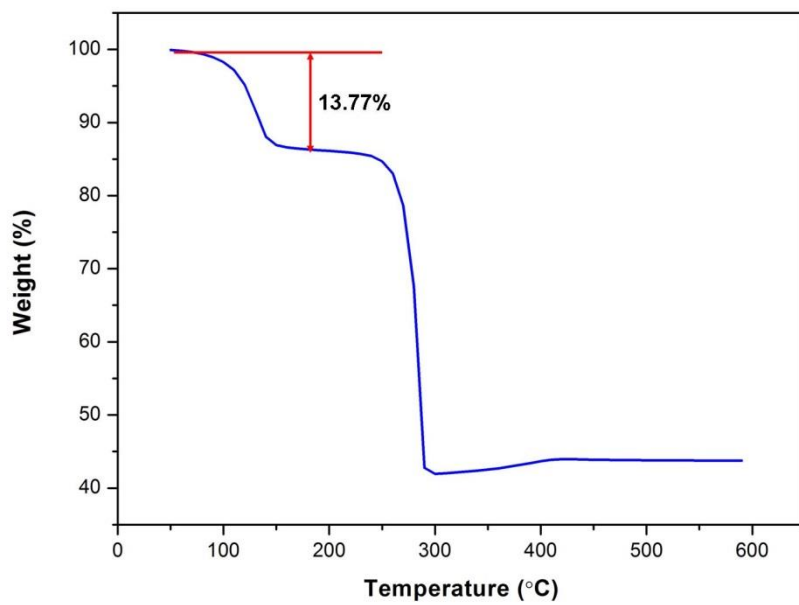
Figure S1. PXRD patterns of (a) $\text{Co}_3(\text{HCOO})_6$, (b) $\text{Ni}_3(\text{HCOO})_6$, (c) $\text{Mn}_3(\text{HCOO})_6$. From bottom to top: simulated (black), as made (red), after gas sorption experiments (blue).

II. Thermal stability

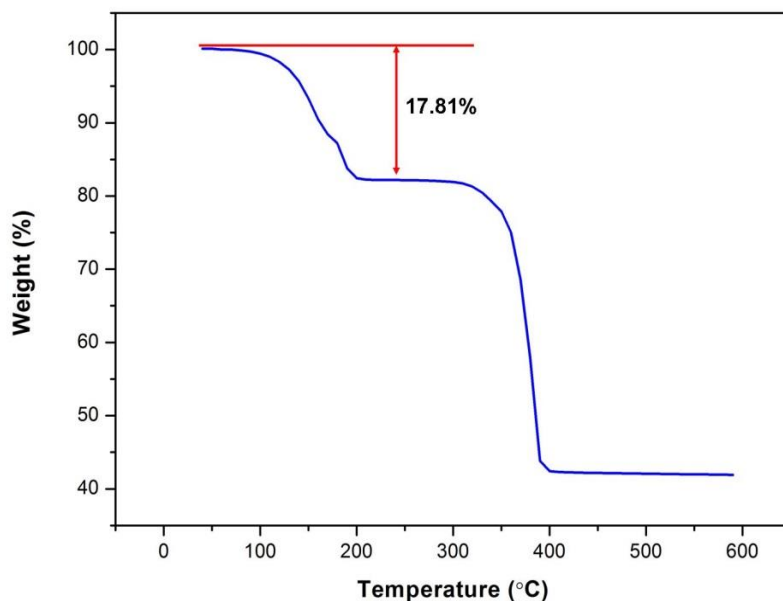
Instrument and method: Thermogravimetric data were collected on a TA Q50 Analyzer with a temperature ramping rate of 10 °C/min from room temperature to 600 °C under nitrogen gas flow.



(a)



(b)



(c)

Figure S2. Thermogravimetric analysis of freshly prepared samples. (a) $\text{Co}_3(\text{HCOO})_6$, (b) $\text{Ni}_3(\text{HCOO})_6$, (c) $\text{Mn}_3(\text{HCOO})_6$. Showing a good agreement between the observed weight loss of solvent DMF and the calculated value (14.03%, 14.01%, and 14.57% for Co, Ni, and Mn respectively).

III. Gas sorption experiments

Instrument and method: Gas sorption experiments at ambient temperatures were performed using a volumetric gas sorption analyzer (Autosorb-1 MP, Quantachrome Instruments). Measurements at cryogenic temperatures were carried out using a high-resolution Micromeritics 3Flex adsorption instrument. The 3Flex (Micromeritics) was equipped with high-vacuum system, three 0.1 Torr pressure transducers, and was coupled with a cryostat (Cold Edge Technologies) that maintains the cryogenic temperatures with a stability in the range of ± 0.001 K from the target temperature. Ultra high purity Xenon, Krypton, Ar and Ne (99.999%) were used. The initial outgassing process for each sample was carried out at 393K overnight (under vacuum). Outgassed samples in the amount of ~ 100 mg were used for gas sorption measurements and the weight of each sample was recorded before and after outgassing to confirm the

removal of guest molecules. The outgassing procedure was repeated on the same sample between experiments for 2~4 hour. Xenon and Krypton sorption isotherms in $M_3(\text{HCOO})_6$ ($M = \text{Ni}$ and Mn) at different temperature are shown in Figure S3.

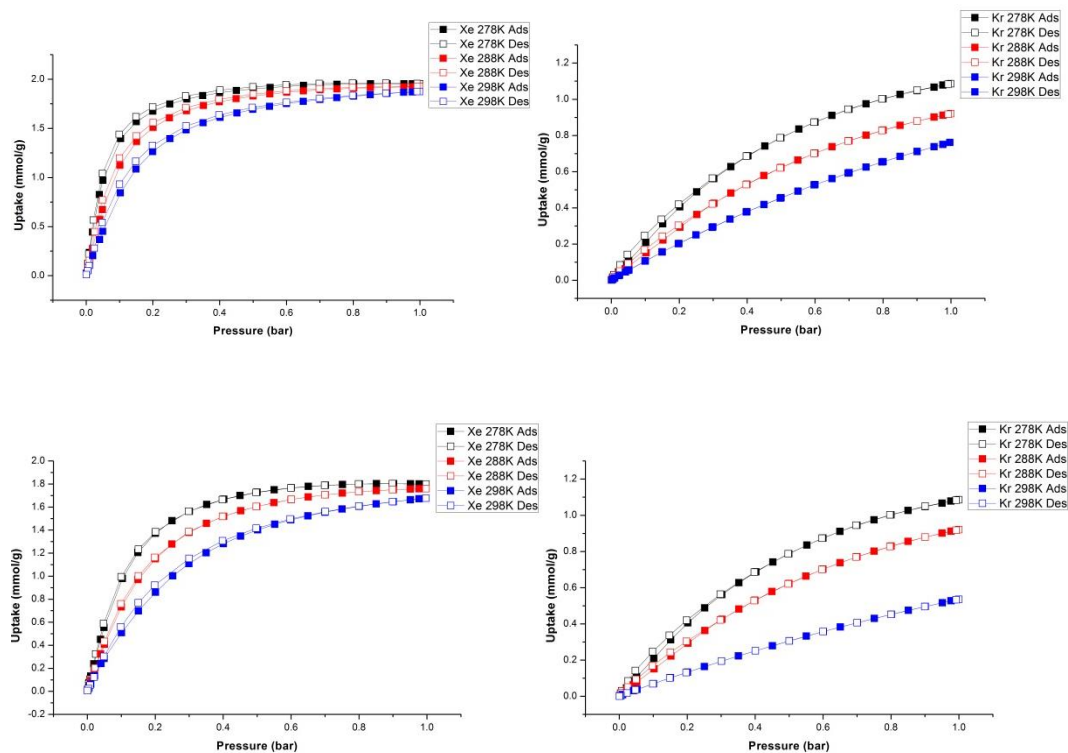


Figure S3. Adsorption and desorption isotherms of Xenon in $\text{Ni}_3(\text{HCOO})_6$ (Top Left); Krypton in $\text{Ni}_3(\text{HCOO})_6$ (Top Right); Xenon in $\text{Mn}_3(\text{HCOO})_6$ (Bottom Left); Krypton in $\text{Mn}_3(\text{HCOO})_6$ (Bottom Right).

Table S1. Summary of xenon adsorption on $M_3(\text{HCOO})_6$ ($M = \text{Co}, \text{Ni}, \text{Mn}$) series

Formula	$\text{Co}_3(\text{HCOO})_6$	$\text{Ni}_3(\text{HCOO})_6$	$\text{Mn}_3(\text{HCOO})_6$
Space group	$P2_1/n$	N/A	$P2_1/n$
V unit cell (\AA^3)	1630.88	N/A	1813.8
Density of as made (g/cm^3)	2.118	N/A	1.860
Density of solvent free (g/cm^3)	1.820	N/A	1.592
Uptake (cc/g) at 298K, 1bar	44.11	41.98	37.56
Uptake (w%) at 298K, 1bar	25.80	24.55	21.97
Uptake (mmol/g) at 298K, 1bar	1.97	1.87	1.68
Uptake (mmol/cm^3) at 298K, 1bar	3.59	N/A	2.67
Uptake (mole/uc) at 298K, 1bar	3.52	N/A	2.91
Uptake (mole/seg) at 298K, 1bar	0.88	N/A	0.73
Uptake (mole/seg) 288K, 1bar	0.89	N/A	0.77

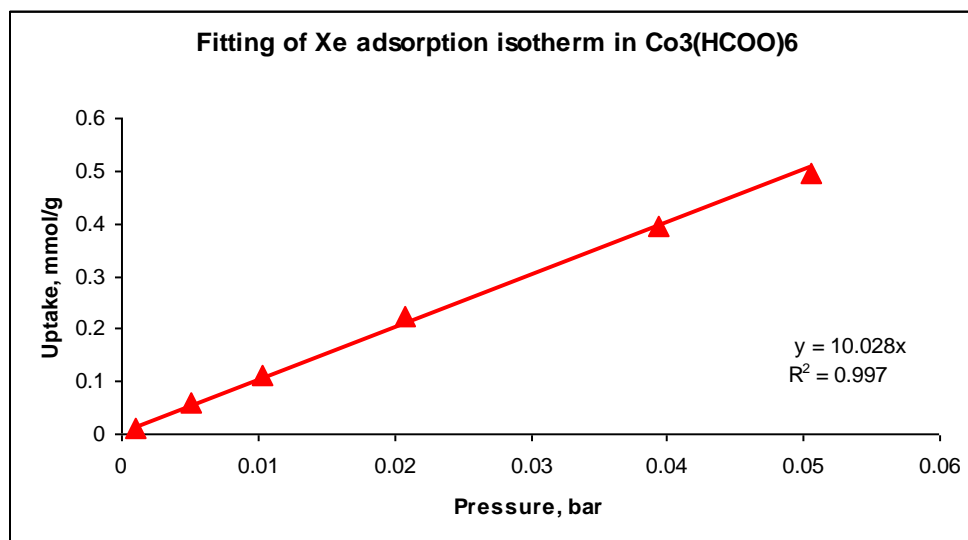
Uptake (mole/seg) 278K, 1bar	0.89	N/A	0.78
------------------------------	------	-----	------

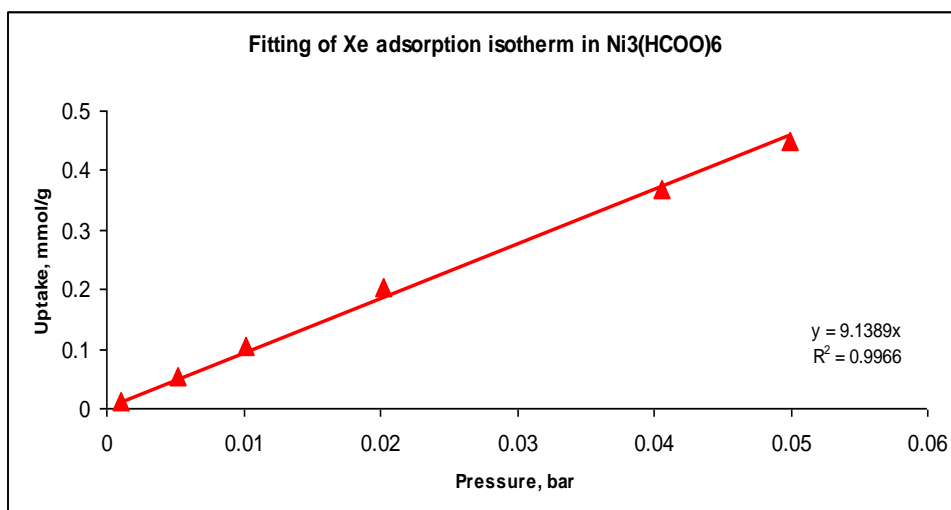
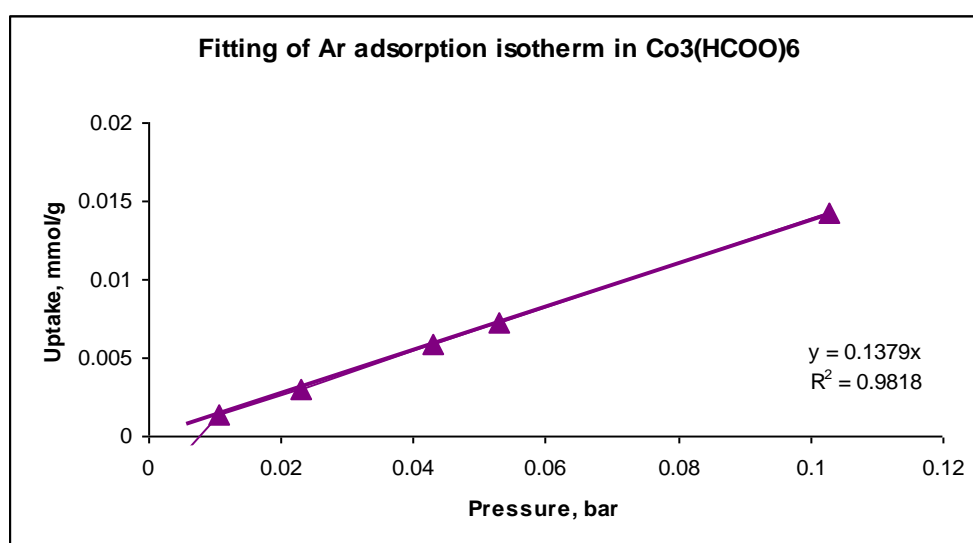
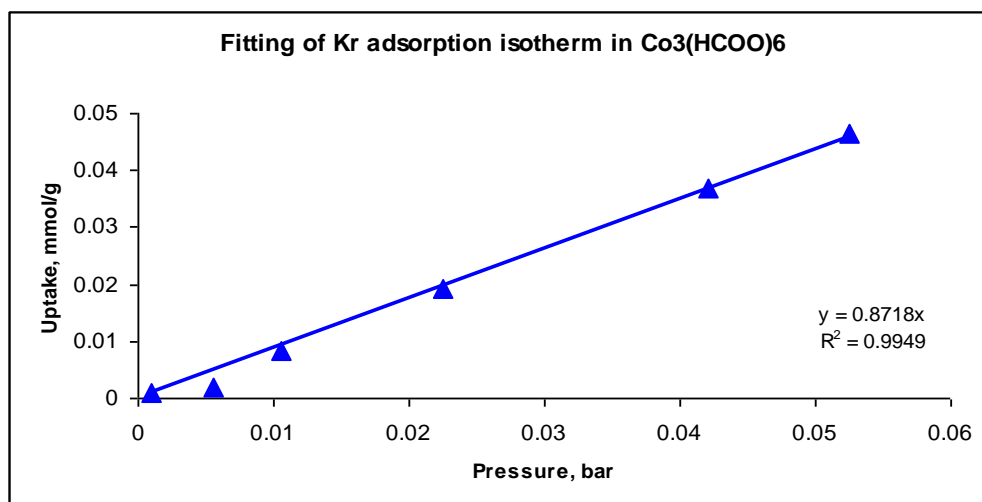
Table S2. Summary of xenon/krypton selectivity in $M_3(\text{HCOO})_6$ ($M = \text{Co}, \text{Ni}, \text{Mn}$) series at 298 K

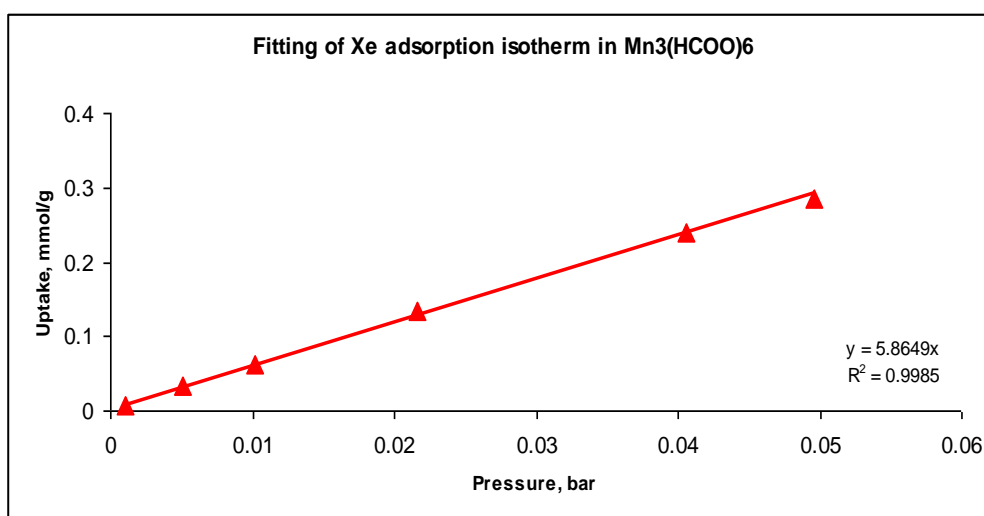
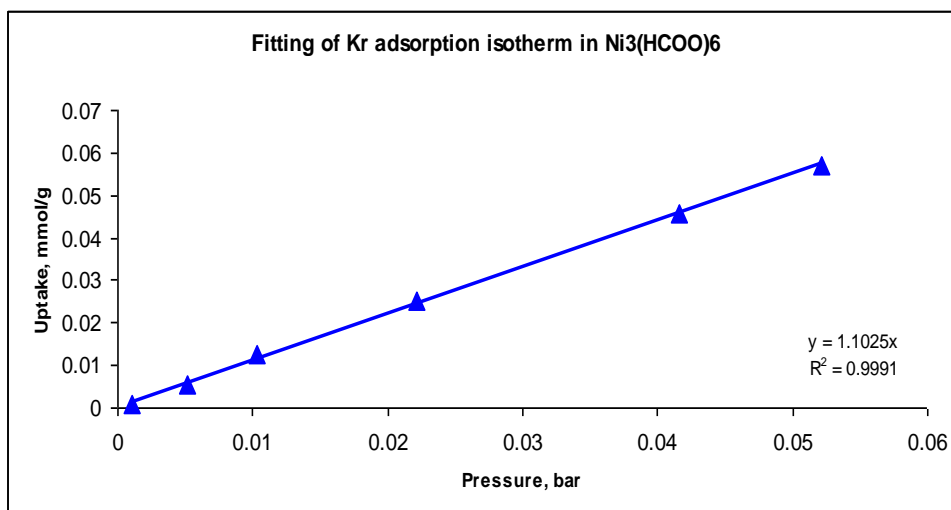
Formula	$\text{Co}_3(\text{HCOO})_6$	$\text{Ni}_3(\text{HCOO})_6$	$\text{Mn}_3(\text{HCOO})_6$
Xe Uptake at 1bar, mmol/g	1.97	1.87	1.68
Kr Uptake at 1bar, mmol/g	0.771	0.761	0.536
Henry's constant of Xe adsorption, mmol/g/bar	10.028	9.139	5.865
Henry's constant of Kr adsorption, mmol/g/bar	0.872	1.102	0.727
Ratio of uptake	2.56	1.70	3.13
Xe/Kr selectivity by the ratio of Henry's constant	11.5	8.3	8.1

IV. Henry's constant fitting

Low pressure range of the adsorption isotherm is nearly linear which corresponds to Henry's law behavior. Thus Henry's constant can be obtained from a linear fit to the initial part of the isotherm. In our case, the fitting is applied to the range where $P < 0.1$ bar to guarantee it is within Henry's region.







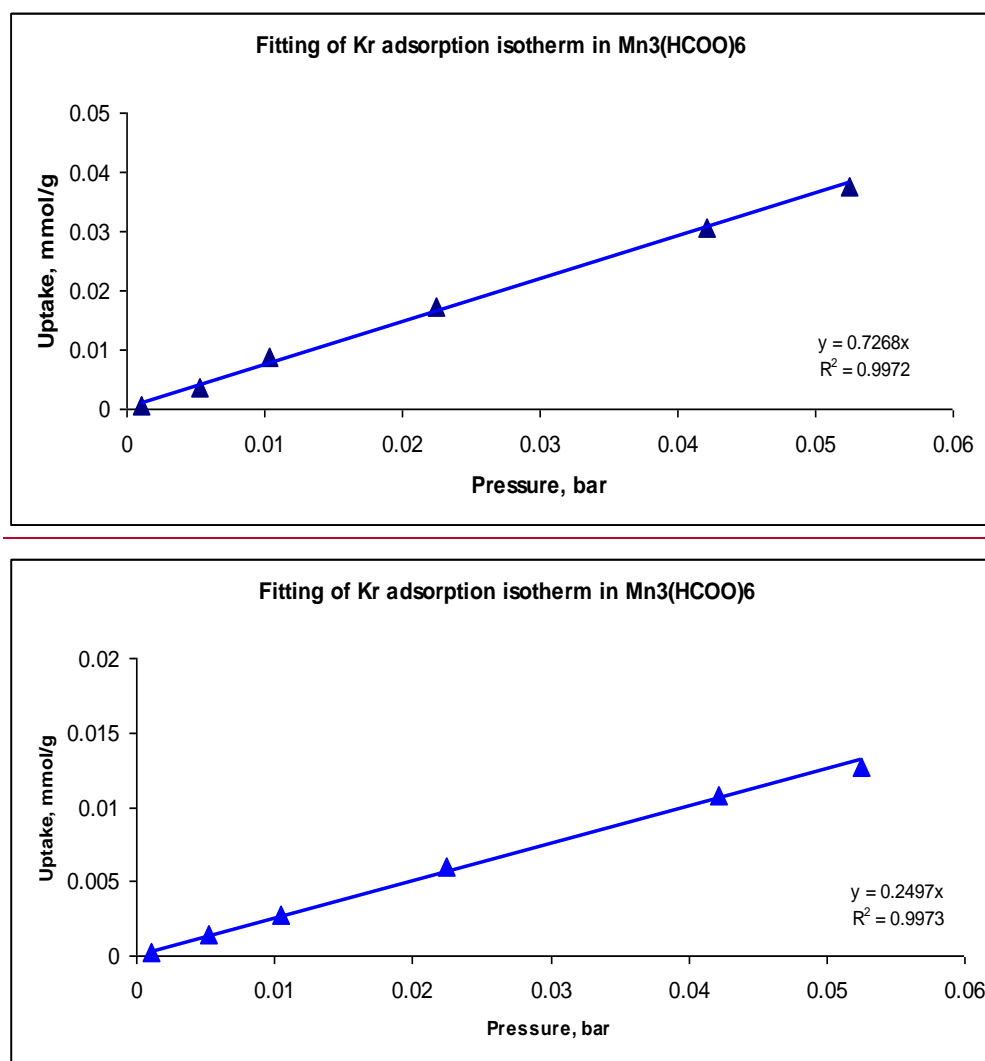


Figure S4. Fitting of Henry's constant.

V. Ideal adsorbed solution theory (IAST) selectivity

The ideal adsorbed solution theory (IAST) developed by Myers and Praunitz¹ assumes that the adsorbed mixture is an ideal solution at constant spreading pressure and temperature, where all the components in the mixture conform to the rule analogous to Raoult's law, and the chemical potential of the adsorbed solution is considered equal to that of the gas phase at equilibrium.

From the IAST, the spreading pressure π is given by

$$\pi_i^0(p_i^0) = \frac{RT}{A} \int_0^{p_i^0} qd \ln p \quad (1)$$

$$\pi^* = \frac{\pi A}{RT} = \int_0^{p_i^0} \frac{q_i}{p} dp \quad (2)$$

Where A is the specific surface area of the adsorbent, π and π^* are the spreading pressure and the reduced spreading pressure, separately. p_i^0 is the gas pressure of component i that corresponding to the spreading pressure π of the gas mixture.

At a constant temperature, the spreading pressure of single component is the same:

$$\pi_1^* = \pi_2^* = \dots = \pi_n^* = \pi \quad (3)$$

The relation between the mole fraction in the gaseous phase y_i , and the mole fraction in the adsorbed phase x_i is described by Raoult's law for ideal solutions,

$$P \times y_i = p_i^0 (\pi^*) x_i \quad (4)$$

Where p_i^0 is the pressure of the single component i in its standard state which is fixed by the spreading pressure of the mixture according to Eq (3). Finally, the total number of moles adsorbed can be obtained from:

$$\frac{1}{q_i} = \sum_i^n \frac{x_i}{q_i^0(p_i^0)} \quad (5)$$

Where $q_i^0(p_i^0)$ is the adsorbed amount from the pure component isotherms.

The selectivity of j over i is

$$S_{ji} = \frac{p_i^0}{p_j^0} = \frac{P y_i / x_i}{P y_j / x_j} = \left(\frac{x_j}{y_j} \right) \left(\frac{y_i}{x_i} \right) \quad (6)$$

Dual Site Langmuir-Freundlich Model for Xe, Kr, and Ar Adsorption Isotherms

The Dual site Langmuir-Freundlich (DSLFL) model² can be expressed as follows:

$$N = N_1^{\max} \times \frac{b_1 p^{1/n_1}}{1 + b_1 p^{1/n_1}} + N_2^{\max} \times \frac{b_2 p^{1/n_2}}{1 + b_2 p^{1/n_2}} \quad (7)$$

Here, p is the pressure of the bulk gas at equilibrium with the adsorbed phase (kPa), N is the adsorbed amount per mass of adsorbent (mol/kg), N_1^{\max} and N_2^{\max} are the

saturation capacities of sites 1 and 2 (mol/kg), b_1 and b_2 are the affinity coefficients of sites 1 and 2 (1/kPa), and n_1 and n_2 represent the deviations from an ideal homogeneous surface. The single-component Xe and Kr adsorption isotherms have been fit to enable the application of IAST in simulating the performance of **1'** under a mixed component gas. The fitting parameters of DSLF equation as well as the correlation coefficients (R^2) are listed in Table S3. The experimental and fitted isotherm for Xe and Kr at 298 K are depicted in Figure S5.

Table S3. Equation parameters for the DSLF isotherm model

Adsorbates	N_1^{\max} (mmol/g)	b_1 (kPa ⁻¹)	n_1	N_2^{\max} (mmol/g)	b_2 (kPa ⁻¹)	n_2	R^2
Xe	0.93	0.11	1.16	1.24	0.018	0.65	0.9999
Kr	0.01	0.00036	0.74	1.92	0.0036	0.88	0.9999
Ar	0.0010	0.00012	0.84	1.11	0.0011	0.96	0.9999

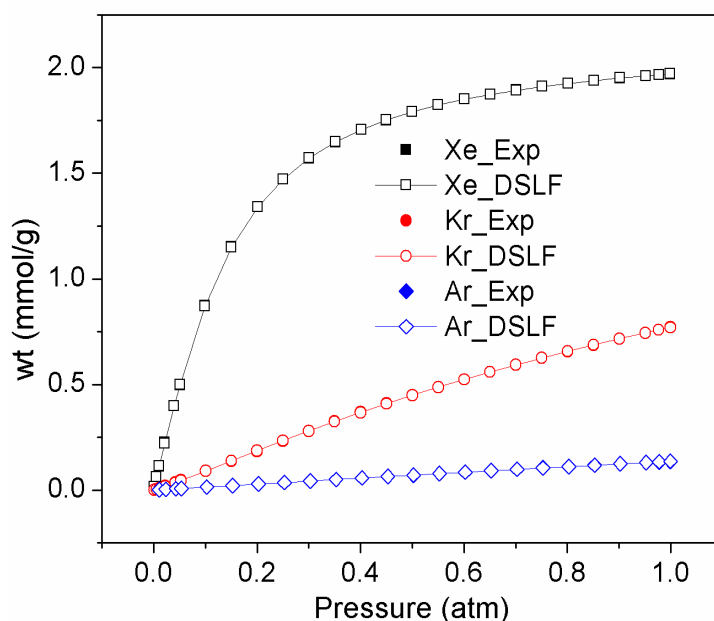


Figure S5. Experimental and fitted isotherms for Xe, Kr and Ar at 298K

VI. Isothermic heats of adsorption (Q_{st}) of noble gases in $\text{Co}_3(\text{HCOO})_6$ measured at cryogenic temperatures

In order to further understand the interactions between atoms of noble gases and the framework, we measured adsorption isotherms of Xe, Kr, and Ar at three temperatures (180, 190, 200 K) and Ne also at three temperatures but in a lower range (80, 90, 100 K) to calculate the isothermic heats of adsorption Q_{st} of these noble gases. The isothermic heats of adsorption (Q_{st}) can be obtained by using the virial equation.³

$$\ln(p) = \ln(v) + (1/T) \sum_{i=0}^m a_i v^i + \sum_{j=0}^n b_j v^j \quad (8)$$

where v , p , and T are amount adsorbed, pressure, and temperature, respectively. Fitting equation (6) to adsorption data measured at different temperatures gives a set of temperature independent parameters a_i and b_i which are used in direct evaluation of Q_{st}

$$Q_{st} = -R \sum_{i=0}^m a_i v^i \quad (9)$$

Where R is the universal gas constant.

Experimental adsorption isotherms of Xe, Kr, and Ar measured on $\text{Co}_3(\text{HCOO})_6$ sample and the goodness of fit by curves fitted by equation (6) are shown in Figures S6 – S8.

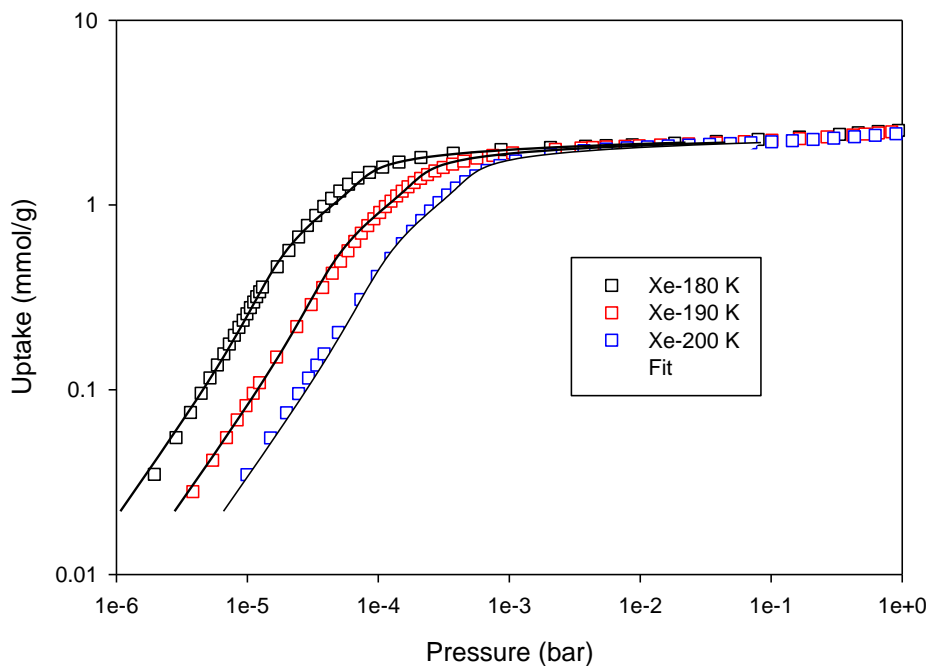


Figure S6. Xenon adsorption isotherms measured at 180, 190 and 200 K on $\text{Co}_3(\text{HCOO})_6$ and their fit by equation 8.

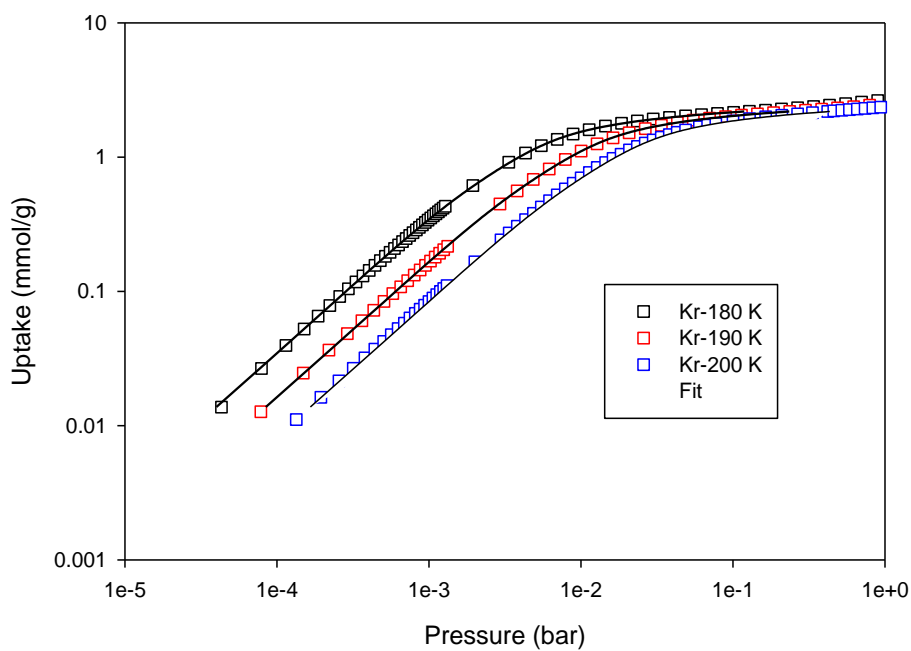


Figure S7. Krypton adsorption isotherms on $\text{Co}_3(\text{HCOO})_6$ and their fit by equation 8.

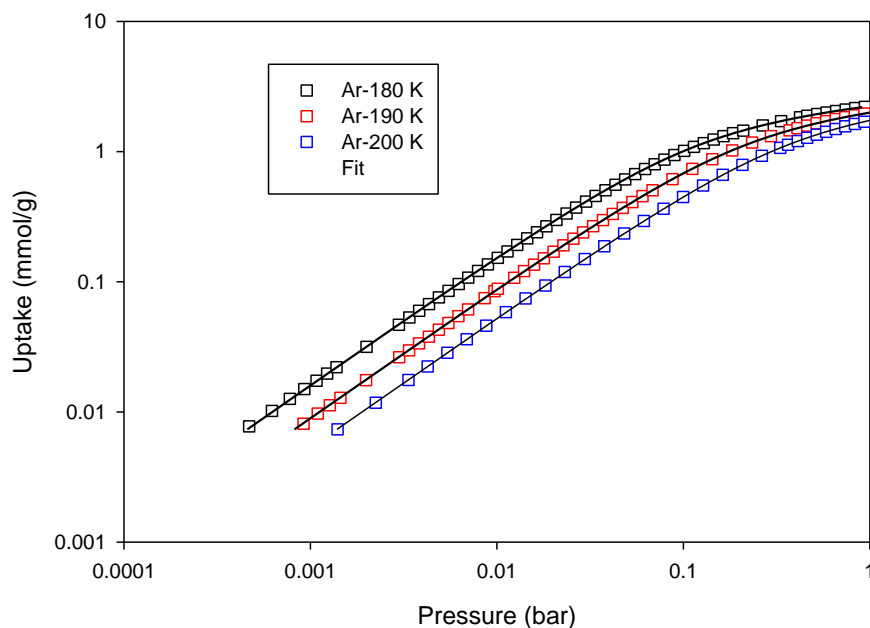


Figure S8. Argon adsorption isotherms on $\text{Co}_3(\text{HCOO})_6$ and their fit by equation 8.

Table S4. Empirical parameters from fitting of virial equation

	Xe	Kr	Ar
a0	-3.26E+03	-2.56E+03	-2.00E+03
a1	-1.36E+02	-2.15E+02	4.43E-01
a2	-5.39E+02	2.85E+02	-1.62E+00
a3	1.46E+03	-2.34E+02	1.96E+01
a4	-1.13E+03	7.79E+01	
a5	2.87E+02		

VII. Breakthrough experiments

In a typical breakthrough experiment, ~500 mg of MOF sorbent was gently ground and packed into a quartz column (5.8 mm I.D. × 150 mm) with silica wool filling the void space. The sorbent was in situ activated in the column with a helium flow (10 mL min⁻¹) at 150 °C for 2 h before the temperature of the column was decreased to 25 °C. The flow of He was then turned off while a gas mixture of Kr/Xe (90:10, v/v) at 10.0 mL

min^{-1} was sent into the column. The effluent from the column was monitored using a mass spectrometer (MS). The dead time was determined using the same column after adsorption saturation. Breakthrough times were calculated by subtracting the dead time from the observed breakthrough time (Figure S9).

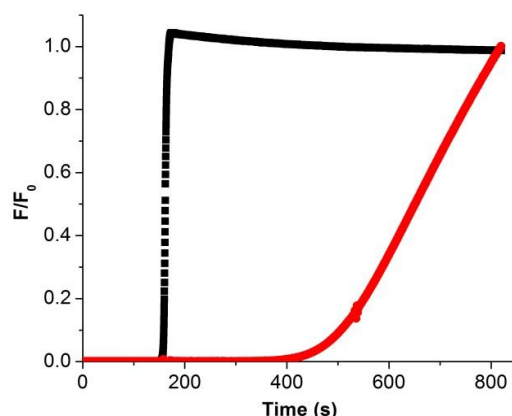


Figure S9. Column breakthrough experiment for Xe/Kr:10/90 binary gas system at 298 K and 1 bar in $\text{Co}_3(\text{HCOO})_6$, (Black): Kr and (Red): Xe.

References:

1. A. L. Myers and J. M. Prausnitz, *AIChE Journal*, 1965, **11**, 121-127.
2. (a) G. Arora and S. I. Sandler, *J. Chem. Phys.*, 2005, **123**; (b) R. Babarao, Z. Hu, J. Jiang, S. Chempath and S. I. Sandler, *Langmuir*, 2006, **23**, 659-666; (c) Y.-S. Bae, O. K. Farha, A. M. Spokoyny, C. A. Mirkin, J. T. Hupp and R. Q. Snurr, *Chemical Communications*, 2008, **0**, 4135-4137; (d) Y.-S. Bae, K. L. Mulfort, H. Frost, P. Ryan, S. Punnathanam, L. J. Broadbelt, J. T. Hupp and R. Q. Snurr, *Langmuir*, 2008, **24**, 8592-8598; (e) Z. Zhang, Z. Li and J. Li, *Langmuir*, 2012, **28**, 12122-12133.
3. (a) L. Czepirski and J. JagiełŁo, *Chemical Engineering Science*, 1989, **44**, 797-801; (b) J. JagiełŁo, T. J. Bandosz and J. A. Schwarz, *Langmuir*, 1996, **12**, 2837-2842; (c) B. Chen, X. Zhao, A. Putkham, K. Hong, E. B. Lobkovsky, E. J. Hurtado, A. J. Fletcher and K. M. Thomas, *Journal of the American Chemical Society*, 2008, **130**, 6411-6423.